Role of endoplasmic reticulum oxidase 1α in H9C2 cardiomyocytes following hypoxia/reoxygenation injury

LINA LAI[1], YUE LIU[2,3], YUANYUAN LIU[2,4], NI ZHANG[2], SHILU CAO[2,5], XIAOJING ZHANG[1] and DI WU[6]

Departments of [1]Pharmacology and [2]Clinical Medicine, Changzhi Medical College, Changzhi, Shanxi 046000; [3]Department of Internal Medicine, Tianjin Medical University, Tianjin 300202; [4]Department of Biochemistry and Molecular Biology, Jinzhou Medical University, Jinzhou, Liaoning 121001; [5]Department of Internal Medicine, Northwest Minzu University, Yinchuan, Ningxia 750011, P.R. China; [6]Department of Surgery, University of Virginia, Charlottesville, VA 22908, USA

Received September 28, 2019; Accepted March 30, 2020

DOI: 10.3892/mmr.2020.11217

Abstract. Endoplasmic reticulum (ER) oxidase 1α (ERO1α) is a glycosylated flavoenzyme that is located on the luminal side of the ER membrane, which serves an important role in catalyzing the formation of protein disulfide bonds and ER redox homeostasis. However, the role of ERO1α in myocardial hypoxia/reoxygenation (H/R) injury remains largely unknown. In the present study, ERO1α expression levels in H9C2 cardiomyocytes increased following H/R, reaching their highest levels following 3 h of hypoxia and 6 h of reoxygenation. In addition, H/R induced apoptosis, and significantly increased expression levels of ER stress (ERS) markers 78 kDa glucose-regulated protein and C/EBP homologous protein. Moreover, the genetic knockdown of ERO1α using short hairpin RNA suppressed cell apoptosis, caspase-3 activity, expression levels of cleaved caspase-12 and cytochrome c in the cytoplasm. Overall, this suggested that ERO1α knockdown may protect against H/R injury. The ERS activator tunicamycin (TM) was used to counteract the ERO1α-induced reduction in ERS; however, the percentage of apoptotic cells and the level of mitochondrial damage did not change. In conclusion, the results from the present study suggested that ERO1α knockdown may protect H9C2 cardiomyocytes from H/R injury through inhibiting intracellular ROS production and increasing intracellular levels of Ca^{2+}, suggesting that ERO1α may serve an important role in H/R.

Correspondence to: Professor Lina Lai, Department of Pharmacology, Changzhi Medical College, 161 Jiefang East Street, Changzhi, Shanxi 046000, P.R. China
E-mail: lailina@126.com

Key words: hypoxia/reoxygenation, endoplasmic reticulum oxidase 1α, apoptosis, endoplasmic reticulum stress, reactive oxygen species

Introduction

Prompt reperfusion is essential for recovery following acute myocardial infarction; however, reperfusion can also lead to ischemia/reperfusion (I/R) injury (1). Although myocardial I/R injury involves complex pathophysiological mechanisms that have not yet been fully elucidated, oxidative stress and intracellular Ca^{2+} overload are considered to be two of the main mechanisms contributing to myocardial I/R injury (2-4). Increases in reactive oxygen species (ROS) and intracellular Ca^{2+} levels are described as mutually causative, forming a vicious cycle (5). Intracellular Ca^{2+} homeostasis and ROS production are closely related to the endoplasmic reticulum (ER) and mitochondria. When faced with oxidative stress, ischemia, hypoxia, Ca^{2+} imbalance and other conditions, unfolded proteins accumulate in the (ER), and upon exceeding its capacity to deal with unfolded proteins, ER homeostasis is lost and the ER stress (ERS) response is activated (6). Accumulating studies have reported that ERS serves an important role in myocardial I/R injury (7,8).

The ER is associated with the mitochondria at multiple levels through mitochondrial-associated membranes (MAMs), which are specific protein-rich regions of the ER located in close proximity to the mitochondria. MAMs regulate several functions, including the synthesis and transport of phospholipids, Ca^{2+} transfer between organelles and cell signaling pathways (9-11). ER oxidase 1 (ERO1) is a glycosylated flavonase located at MAMs, of which there are two mammalian isoforms; the ERO1α isotype, which is found distributed throughout the body, and the ERO1β isotype, which is most abundant in pancreatic β cells and lymphocytes (12,13). Both isoforms respond to ERS, but only ERO1α is induced by hypoxia (14,15). ERO1α serves an important role in catalyzing the formation of protein disulfide bonds, ER redox and Ca^{2+} homeostasis (16), and the ERO1α-dependent ER-mitochondrial calcium flux has been observed to contribute to ERS (17). However, the exact role of ERO1α in myocardial I/R injury remains unclear.

In the present study, myocardial I/R injury was simulated using myocardial hypoxia/reoxygenation (H/R). The effects of ERO1α on myocardial H/R were observed by genetically

knocking down the expression of ERO1α with short hairpin RNA (shRNA), and treatment with the ERS activator, TM or the ERS inhibitor, 4-Phenylbutyric acid (4-PBA).

Materials and methods

Lentiviral cell transfection. Using the ERO1α gene mRNA sequence (GenBank accession no. NM_138528.1), three shRNA candidate target sequences (1832, 1833 and 1834) were designed and synthesized by Shanghai GeneChem Co., Ltd. The above target sequences were cloned into the lentiviral vector pMAGic4.1 and scrambled shRNA was cloned into the pMAGic4.1 vector as the negative control. H9C2 cells (American Type Culture Collection) were plated in 6-well plates at a density of $1x10^6$ cells/well, and upon reaching 70% confluence, the cells were transfected with either recombinant lentivirus ERO1α-shRNA (Table I) or scrambled shRNA with titers of $5x10^6$ TU/ml. Following transfection for 48 h, the efficiency of ERO1α silencing was assessed using reverse transcription-quantitative PCR and western blotting. The shRNA with the best silencing effect was selected for subsequent experiments.

Exposure of H9C2 cardiomyocytes to H/R and treatments. H9C2 cardiomyocytes were purchased from the American Type Culture Collection and the H/R model was established using the AnaeroPack® method (18). Briefly, a hypoxic atmosphere was created by incubating an AnaeroPack® (Mitsubishi Gas Chemical Company, Inc.), which absorbs oxygen, and H9C2 cardiomyocytes in a sealed airtight container together at 37˚C. Following incubation for 3 h, the AnaeroPack® container was opened to terminate the hypoxic conditions. The cells in the culture plates were removed and subsequently placed in a CO_2 incubator at 37˚C for 6 h. The morphology was observed under an inverted light microscope at x200 magnification. In the 4-PBA + H/R group, H9C2 cardiomyocytes were treated with 0.5 mM 4-PBA (Sigma-Aldrich; Merck KGaA), a selective ERS inhibitor, 2 h prior to H/R induction. In the TM + ERO1α-shRNA + H/R, cardiomyocytes were pretreated with 2 μg/l TM (Cayman Chemical), an ERS activator, 24 h prior to H/R exposure to counteract the reduction in ERS following ERO1α knockdown.

Morphological analysis following Hoechst 33258 staining. A total of $1x10^5$ H9C2 cardiomyocytes/well were incubated in 24-well plates. Cells were fixed by 4% paraformaldehyde at 4˚C for 1 h, washed twice with PBS and stained with Hoechst 33258 (Beyotime Institute of Biotechnology) at room temperature for 5 min. Hoechst 33258 staining solution was subsequently aspirated and washed twice with PBS for 5 min each. Stained cell nuclei were visualized using an IX70 fluorescence microscope (Olympus Corporation) (magnification, x200). A total of five fields were randomly selected from each well, and the proportion of apoptotic cells was calculated as the ratio of nuclear pyknosis cells to the total cells.

Flow cytometric analysis of apoptosis. The Annexin V-FITC Apoptosis Assay kit (Beyotime Institute of Biotechnology) was used to detect cell apoptosis. Briefly, following treatment, cells were transferred to individual tubes and a solution containing 195 μl binding buffer, 5 μl Annexin V-FITC and 10 μl propidium iodide was added to each test tube. The tubes were subsequently mixed and incubated at room temperature in the dark for 15 min. Apoptotic cells were detected using a FACSScan flow cytometer (FACSVerse; BD Biosciences). The data analysis was conducted using CellQuest software version 3.3 (BD Biosciences).

Detection of caspase-3 activity. Caspase-3 activity was measured using a caspase-3 activity kit (Beyotime Institute of Biotechnology). Briefly, cells were suspended in lysis buffer on ice for 15 min and subsequently centrifuged at 16,000 x g for 10 min. The supernatants were then incubated with 20 ng Ac-DEVD-pNA in a 96-well plate for 2 h at 37˚C (19). The absorbance of pNA was measured at 405 nm using an Infinite® 200 PRO microplate reader (Tecan Group, Ltd.).

Measurement of intracellular Ca^{2+} levels. Cells were washed twice with PBS buffer and then incubated with Fluo-3/AM working fluid for 30 min in the dark at 37˚C. The fluorescence intensity was determined using a confocal laser scanning microscope (TCS SP5; Leica Microsystems GmbH), with an excitation wavelength of 488 nm and an emission wavelength of 525 nm (magnification, x400). A total of five fields were randomly selected from each dish. Semi-quantitative analysis was conducted using ImageJ 1.49 software (National Institutes of Health).

Measurement of intracellular ROS levels. Intracellular ROS levels were detected by ROS fluorescent probe dichlorodihydrofluorescein diacetate (DCFH-DA). Briefly, $1x10^6$ H9C2 cardiomyocytes/ml were incubated with 10 μM DCFH-DA at 37˚C for 30 min and then washed three times with PBS buffer. The fluorescent intensity was detected with an excitation wavelength of 488 nm and an emission wavelength of 525 nm using an Infinite® 200 PRO microplate reader (Tecan Group, Ltd.). The results represent the percentage variation relative to the untreated control.

Extraction of the cytoplasmic and mitochondrial components. The cytoplasmic and mitochondrial proteins were extracted using a cell mitochondria isolation kit (Beyotime Institute of Biotechnology). Briefly, cells were incubated in lysis buffer at 4˚C and centrifuged at 3,000 x g for 10 min. Subsequently, the supernatants were centrifuged for a second time at 4˚C for 10 min at 13,000 x g. The cytoplasmic components were present in the supernatant, whereas the cell pellet contained the mitochondrial components.

Measurement of mitochondrial membrane potential ($\Delta\psi m$). A total of 100 μl (1 mg/ml) purified mitochondria was added to 900 μl JC-1 staining solution and subsequently incubated at 37˚C for 30 min. To detect the JC-1 monomer, the excitation and emission wavelength was set to 490 and 530 nm, respectively. To detect the JC-1 polymer, the excitation and emission wavelength was set to 525 and 590 nm, respectively (20). The fluorescent intensity was determined using an Infinite® 200 PRO microplate reader (Tecan Group, Ltd.).

Reverse transcription-quantitative PCR (RT-qPCR). Total RNA was extracted using TRIzol® reagent (Takara Bio,

Table I. Short hairpin RNA primer sequences.

ID	Primer sequence (5'→3')
1832	F: ccggGACCATCGATAAGTTTAATAActcgagATTAAACTTATCGATGGTCTCttttttg
	R: aattcaaaaaaGAGACCATCGATAAGTTTAATctcgagTTATTAAACTTATCGATGGTC
1833	F: ccggGAGCATTCTACAGGCTTATATctcgagATAAGCCTGTAGAATGCTCTCttttttg
	R: aattcaaaaaaGAGAGCATTCTACAGGCTTATctcgagATATAAGCCTGTAGAATGCTC
1834	F: ccggGTGGACGAAACACGATGATTCctcgagATCATCGTGTTTCGTCCACTGttttttg
	R: aattcaaaaaaCAGTGGACGAAACACGATGATctcgagGAATCATCGTGTTTCGTCCAC

F, forward; R, reverse.

Table II. Primer sequences used for reverse transcription-quantitative PCR.

Gene	Primer sequence (5'→3')	PCR conditions
ERO1α	F: TGTGCTGTCAAACCCTGCCA	Denaturation, 95˚C, 30 sec; annealing, 57˚C, 20 sec; extension,
	R: CAGCCTGCTCACACTCCTCA	72˚C, 1 min; 35 cycles
GRP78	F: AAGGAAACTGCCGAGGCGTA	Denaturation: 95˚C, 30 sec; annealing, 56˚C, 20 sec; extension,
	R: AAGGAAACTGCCGAGGCGTA	72˚C, 1 min; 35 cycles
CHOP	F: TCCTGAGTGGCGGACTGTTC	Denaturation, 95˚C, 30 sec; annealing, 57˚C, 20 sec; extension,
	R: GGCAGAGACTCAGCTGCCAT	72˚C, 1 min; 35 cycles
Cytochrome c	F: TGGTCTGTTTGGGCGGAAGA	Denaturation, 95˚C, 30 sec; annealing, 57˚C, 20 sec; extension,
	R: TGGTCTGTTTGGGCGGAAGA	72˚C, 1 min; 35 cycles
Caspase-12	F: TGGAGAAGGAAGGCCGAACC	Denaturation, 95˚C, 30 sec; annealing, 57˚C, 20 sec; extension,
	R: TGGACGGCCAGCAAACTTCA	72˚C, 1 min; 35 cycles
18s	F: CGGCTACCACATCCAAGGAA	Denaturation, 95˚C, 30 sec; annealing, 61.5˚C, 20 sec; extension,
	R: GCTGGAATTACCGCGGCT	72˚C, 1 min; 35 cycles

ERO1α, endoplasmic reticulum oxidase 1α; GRP78, 78 kDa glucose-regulated protein; CHOP, C/EBP homologous protein; F, forward; R, reverse.

Inc.). Total RNA was reverse transcribed into cDNA using the PrimeScript RT reagent kit (Takara Bio, Inc.). qPCR was subsequently performed using the SYBR® Premix Ex Taq™ kit (Takara Bio, Inc.), according to the manufacturer's protocol, and a qTower2.2 quantitative PCR instrument (21). Primer sequences of the genes used for the qPCR are presented in Table II. Relative expression of genes was calculated using the comparative cycle threshold (Ct) ($2^{-\Delta\Delta Ct}$) method with 18s RNA as the internal control (22).

Western blotting. Total cell proteins were extracted using RIPA Lysis Buffer (Beyotime Institute of Biotechnology). Mitochondria proteins were extracted using the Cell Mitochondria Isolation kit (Beyotime Institute of Biotechnology) according to the manufacturer's protocol. Protein concentration was determined via BCA protein assay kit (Beyotime Institute of Biotechnology). A total of 50 μg of extracted protein were electroblotted onto a PVDF membrane following separation on a 10% SDS-PAGE. The membranes were blocked with 5% non-fat milk for 1 h at room temperature prior to being incubated with the following primary antibodies overnight at 4˚C: Anti-ERO1α (1:1,000; cat. no. sc-365526) purchased from Santa Cruz Technology, and anti-78 kDa glucose-regulated protein (GRP78; 1:2,000; cat. no. ab108615), anti-C/EBP homologous protein (CHOP; 1:2,000; cat. no. ab179823), anti-caspase-12 (1:2,000; cat. no. ab62484), anti-cytochrome c (1:2,000; cat. no. ab133504) anti-cytochrome c oxidase subunit IV (COX IV; 1:2,000; cat. no. ab153709) and anti-GAPDH (1:5,000; cat. no. ab181602) purchased from Abcam. Following the primary antibody incubation, membranes were washed three times with wash buffer and incubated with horseradish peroxidase-conjugated IgG secondary antibodies (1:2,000; cat. nos. A0208 and A0216, respectively; Beyotime Institute of Biotechnology) for 2 h at room temperature. Protein bands were visualized using an enhanced chemiluminescence system (Beyotime Institute of Biotechnology), with GAPDH as the loading control (COX IV was used as a mitochondrial loading control). Semi-quantitative analysis was conducted using ImageJ 1.49 software (National Institutes of Health).

Statistical analysis. Statistical analysis was performed using SPSS version 19.0 software (IBM Corp.) and data are presented as the mean ± SD. To determine statistical differences amongst >2 groups, one-way ANOVA was used, followed by Tukey's

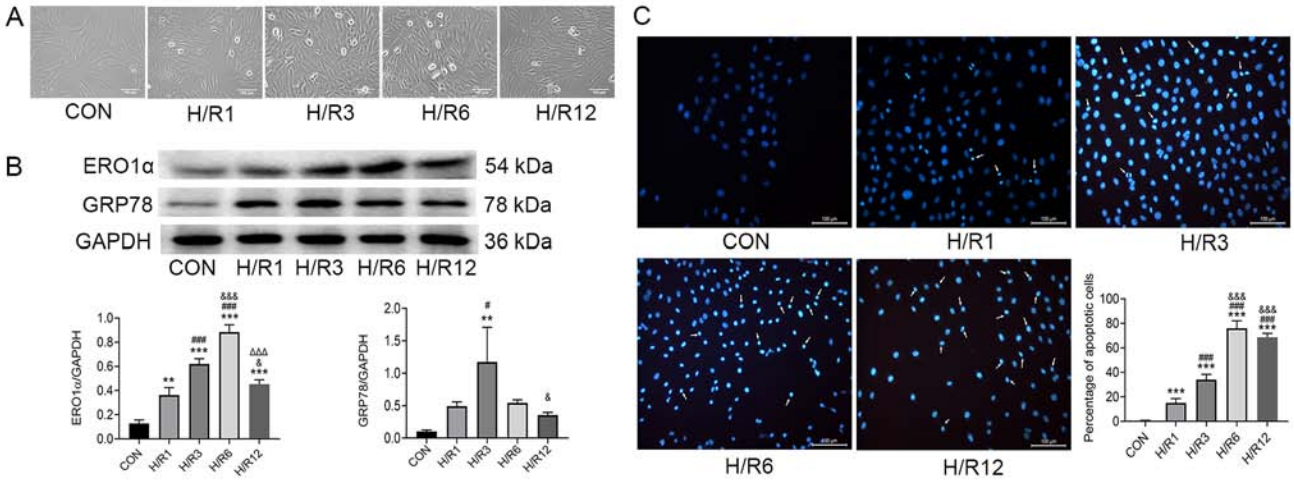

Figure 1. H9C2 cardiomyocytes exposed to hypoxia for 3 h and subsequently 1, 3, 6 and 12 h of reoxygenation. (A) Optical images of H9C2 cardiomyocytes. (B) Protein expression levels of ERO1α and GRP78 as determined by western blot analysis. (C) Apoptosis detected by Hoechst 33258 staining. Scale bar, 100 μm. Data are presented as the mean ± SD from three independent experiments. **P<0.01, ***P<0.001 vs. CON group; $^{\#}$P<0.05, $^{\#\#\#}$P<0.001 vs. H/R1 group; $^{\&}$P<0.05, $^{\&\&\&}$P<0.001 vs. H/R3 group; $^{\Delta\Delta\Delta}$P<0.001 vs. H/R6 group. ERO1α, endoplasmic reticulum oxidase 1α; GRP78, 78 kDa glucose-regulated protein; CON, control; H/R, hypoxia/reoxygenation.

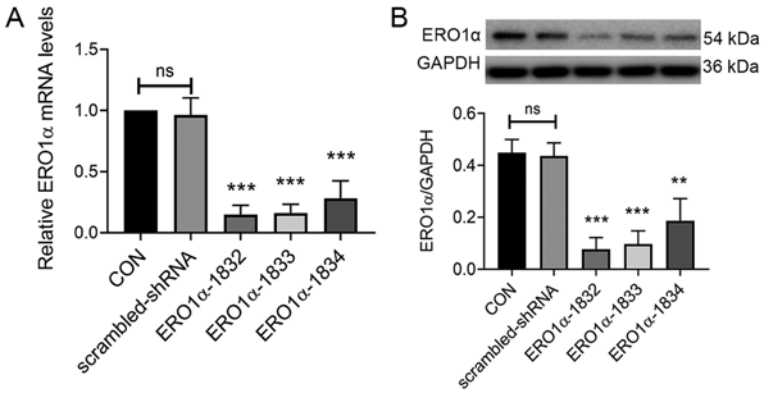

Figure 2. Transfection of shRNA against ERO1α decreases ERO1α expression levels in H9C2 cardiomyocytes. (A) Expression levels of ERO1α mRNA were determined using reverse transcription-quantitative PCR. Results were expressed as the fold change over the CON group. ***P<0.001 vs. CON group. (B) Expression levels of ERO1α protein were determined following transfection for 48 h by western blotting. Data are presented as the mean ± SD from three independent experiments. **P<0.01, ***P<0.001 vs. CON group. shRNA, short hairpin RNA; ERO1α, endoplasmic reticulum oxidase 1α; CON, control; ns, not significant.

post hoc test for multiple group comparisons. P<0.05 was considered to indicate a statistically significant difference.

Results

Expression levels of ERO1α protein increase following H/R induction. H9C2 cardiomyocytes were exposed to hypoxia for 3 h and reoxygenation for 1, 3, 6 and 12 h, and ERO1α protein expression levels were subsequently assessed using western blotting. In the control (CON) group, H9C2 cardiomyocytes did not undergo hypoxia and reoxygenation. The cells in the CON group grew well and most of them were fusiform. Compared with the CON group, hypoxia-reoxygenation caused some cells to appear irregular or round in shape, and floating cells and cell debris increased significantly (Fig. 1A). ERO1α protein expression levels significantly increased following H/R induction compared with the CON group (Fig. 1B); and ERO1α expression levels reached their highest in H9C2 cardiomyocytes following 3 h of hypoxia and 6 h of reoxygenation. In addition, ERS marker GRP78 protein expression levels peaked following 3 h of reoxygenation. Therefore, subsequent experiments in the present study were performed in cells following 3 h of hypoxia and 6 h of reoxygenation.

Consistent with ERO1α expression, H/R-stimulated H9C2 cardiomyocytes demonstrated increased the proportion of apoptotic cells. The nuclei of H9C2 cardiomyocytes in the CON group were round and homogeneously stained, whereas those in the H/R group were observed to have significant apoptotic characteristics, such as cell shrinkage and chromatin condensation (Fig. 1C). Counting the cells with apoptotic characteristics found that the percentage of apoptotic cells in the H/R group was significantly increased compared with the CON group.

Transfection with specific ERO1α-shRNAs decreases ERO1α expression levels in H9C2 cardiomyocytes. The role of ERO1α following H/R was chosen for further investigation because

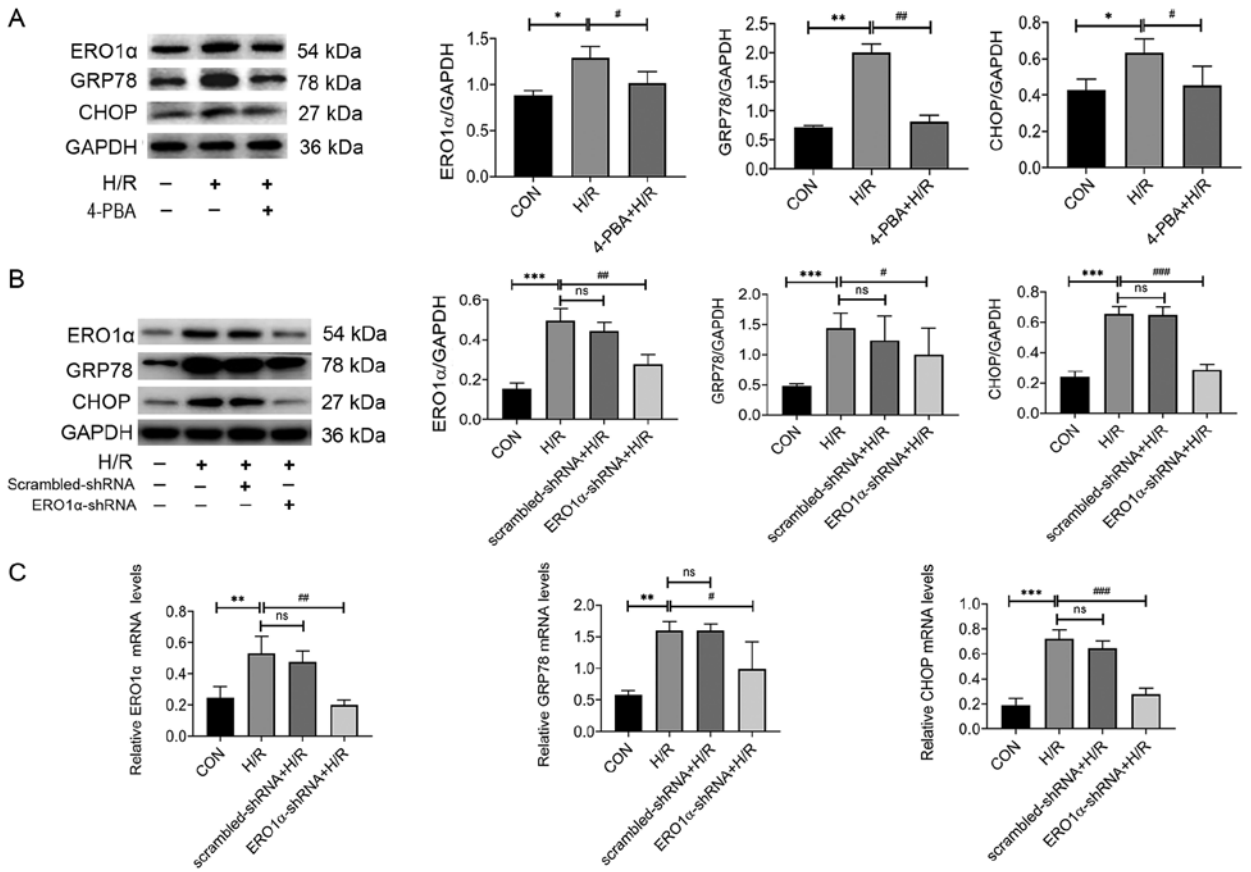

Figure 3. ERO1α knockdown decreases H/R-induced ER stress. (A) Protein expression levels of ERO1α, GRP78 and CHOP in H9C2 cardiomyocytes following pretreatment with 4-PBA for 2 h prior to H/R induction. (B) Protein expression levels of ERO1α, GRP78 and CHOP in ERO1α-shRNA-transfected H9C2 cardiomyocytes. (C) mRNA expression levels of ERO1α, GRP78 and CHOP in H9C2 cardiomyocytes following transfection with ERO1α-shRNA. Data are presented as the mean ± SD from three independent experiments. *P<0.05, **P<0.01, ***P<0.001 vs. CON group; $^{\#}$P<0.05, $^{\#\#}$P<0.01, $^{\#\#\#}$P<0.001 vs. H/R group. ERO1α, endoplasmic reticulum oxidase 1α; GRP78, 78 kDa glucose-regulated protein; CHOP, C/EBP homologous protein; CON, control; H/R, hypoxia/reoxygenation; shRNA, short hairpin RNA; ns, not significant; 4-PBA, 4-Phenylbutyric acid.

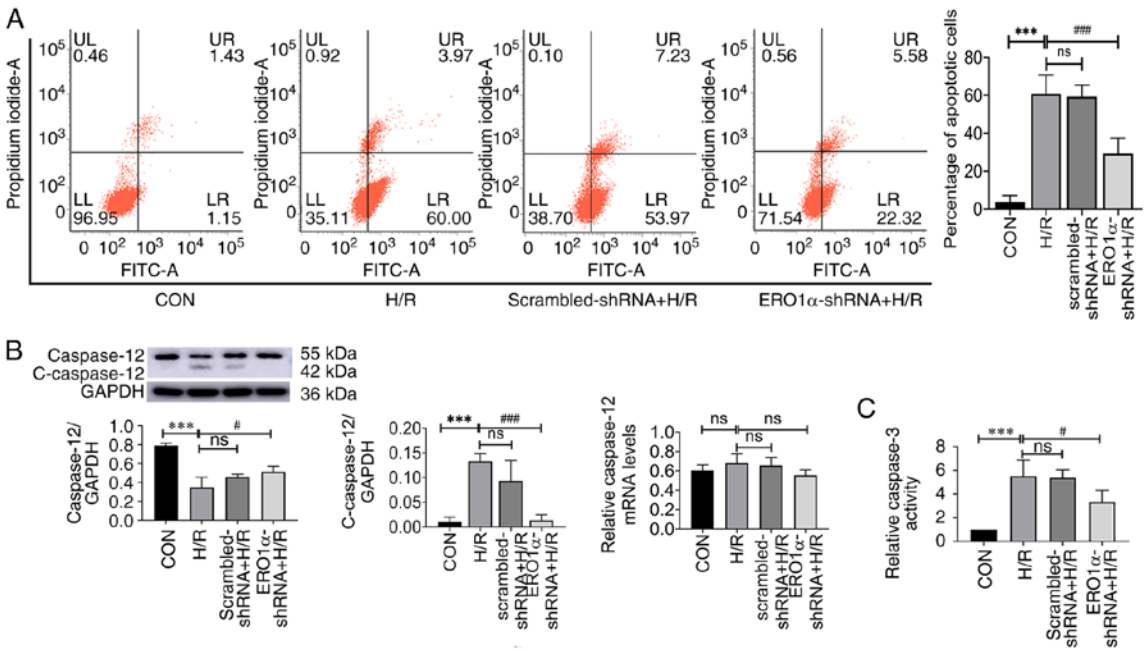

Figure 4. ERO1α knockdown inhibits H/R-induced cell apoptosis. (A) Percentage of apoptotic cells was detected using flow cytometry. (B) Protein expression levels of c-caspase-12 and caspase-12, and the mRNA expression levels of caspase-12 were analyzed using western blotting and reverse transcription-quantitative PCR, respectively. (C) Caspase-3 activity was detected using a caspase-3 activity kit. Data are presented as the mean ± SD from three independent experiments. ***P<0.001 vs. CON group; $^{\#}$P<0.05, $^{\#\#\#}$P<0.001 vs. H/R group. ERO1α, endoplasmic reticulum oxidase 1α; CON, control; H/R, hypoxia/reoxygenation; c, cleaved; shRNA, short hairpin RNA; ns, not significant.

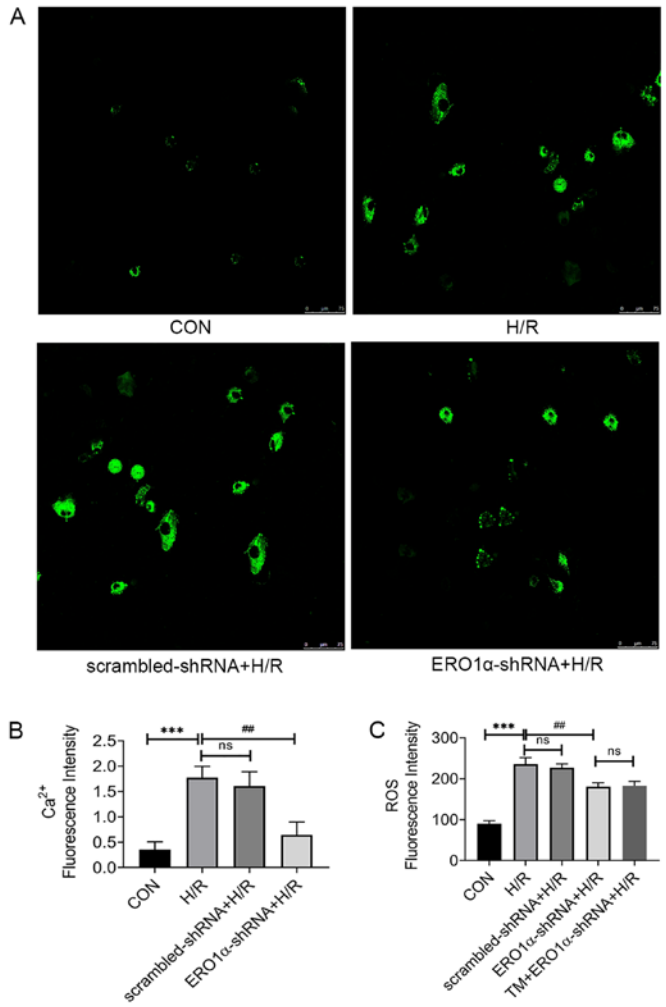

Figure 5. ERO1α knockdown decreases H/R-induced increases in intracellular ROS and Ca^{2+} levels. (A) Intracellular Ca^{2+} levels were detected using a laser scanning confocal microscope. Scale bar, 75 μm. (B) Statistical analysis of the intracellular Ca^{2+} levels are presented in the bar graphs. (C) ROS fluorescence intensity was determined using a microplate reader. Data are presented as the mean ± SD from three independent experiments. ***P<0.001 vs. CON group; $^{\#\#}$P<0.01 vs. H/R group. ROS, reactive oxygen species; ERO1α, endoplasmic reticulum oxidase 1α; CON, control; H/R, hypoxia/reoxygenation; shRNA, short hairpin RNA; ns, not significant; TM, tunicamycin.

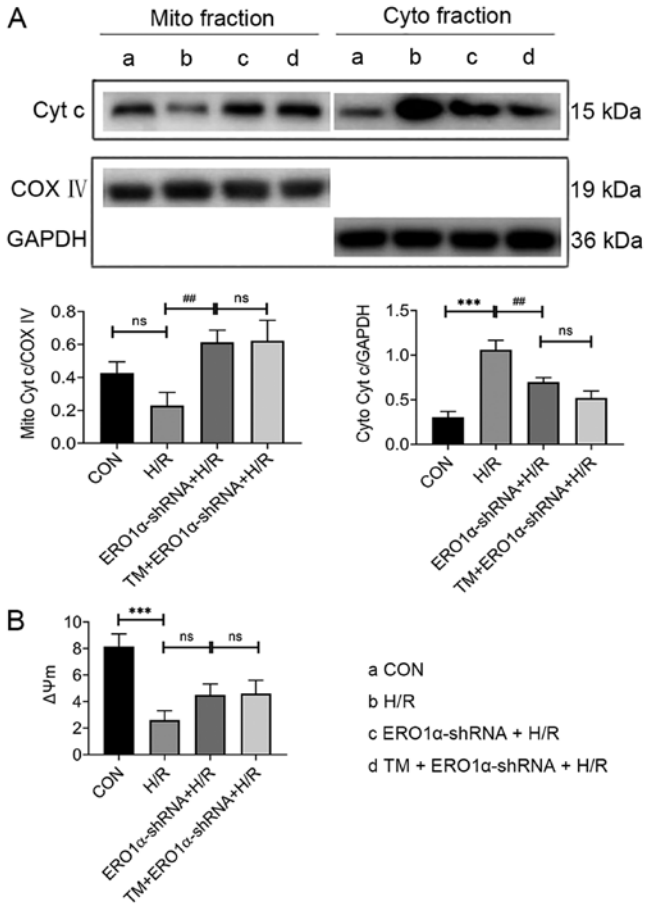

Figure 6. ERO1α knockdown alleviates mitochondrial dysfunction by reducing endoplasmic reticulum stress following H/R injury. (A) Cyt c expression levels in the cytoplasm and mitochondria were analyzed using western blotting. (B) Δψm was detected using a microplate reader following staining with JC-1. Data are presented as the mean ± SD from three independent experiments. ***P<0.001 vs. CON group; $^{\#\#}$P<0.01 vs. H/R group. ERO1α, endoplasmic reticulum oxidase 1α; CON, control; Cyt c, cytochrome c; H/R, hypoxia/reoxygenation; Cyto, cytoplasmic; Mito, mitochondria; COX IV, cyt c oxidase subunit IV; Δψm, mitochondrial membrane potential; shRNA, short hairpin RNA; ns, not significant; TM, tunicamycin.

previous studies had reported that ERS served an important role in myocardial I/R injuries (23,24). ERO1α-shRNA carrier vectors were observed to contain the expected sequence (Table SI), indicating their successful construction. Following transfection of H9C2 cardiomyocytes with three different ERO1α-shRNAs (1832, 1833 and 1834), the mRNA expression levels of ERO1α were significantly decreased in the H9C2 cardiomyocytes (Fig. 2A). Although all three lentiviral shRNAs significantly inhibited ERO1α protein expression (Fig. 2B), the knockdown efficiency of shRNA 1832 was more effective compared with shRNA 1833 and shRNA 1834. Therefore, the lentivirus shRNA 1832 was selected for use in subsequent experiments.

ERO1α knockdown decreases H/R-induced ERS. The mRNA and protein expression levels of ERS-related molecules, including ERO1α, GRP78 and CHOP were detected using RT-qPCR and western blotting. The expression levels of ERO1α, GRP78 and CHOP mRNA and protein significantly increased following H/R compared with the CON group, whereas 4-PBA inhibited the expression levels of ERO1α, GRP78 and CHOP protein (Fig. 3A). Furthermore, ERO1α knockdown reversed the H/R-induced increase in mRNA and protein expression levels of GRP78 and CHOP (Fig. 3B and C). Together, these data strongly suggested that ERS may serve an important role in myocardial H/R injury, and that ERO1α may have a crucial role in H/R-induced ERS in H9C2 cardiomyocytes.

ERO1α knockdown inhibits H/R-induced cell apoptosis. The percentage of apoptotic cells, caspase-3 activity and the expression levels of caspase-12 and cleaved-caspase-12 (c-caspase-12) were investigated to determine the role of ERO1α in H/R injury. H9C2 cardiomyocytes underwent hypoxia for 3 h, then reoxygenation for 6 h, and the percentage of apoptotic cells was evaluated using flow cytometry. The percentage of apoptotic cells in the H/R group was significantly increased compared with the CON group (Fig. 4A); however, the percentage of apoptotic cells of the ERO1α-shRNA + H/R group was decreased compared with the H/R group.

Apoptosis requires the activation of cysteine protease, which both promotes and executes cell death (25). Excessive ERS was reported to induce apoptotic signaling in I/R injury (26). Thus, the expression levels of caspase-12 and c-caspase-12 proteins, and caspase-3 activity were subsequently investigated (Fig. 4B and C). The expression levels of c-caspase-12 in the H/R group were significantly increased compared with the CON group; however, ERO1α knockdown reduced c-caspase-12 expression compared with the H/R group. These data suggested that ERO1α knockdown may inhibit H/R-induced apoptosis in H9C2 cardiomyocytes.

ERO1α knockdown decreases H/R-induced increases in intracellular ROS and Ca^{2+} levels. Under stress conditions, increases in intracellular Ca^{2+} levels promote apoptosis (27), thus the intracellular Ca^{2+} influx in response to H/R was measured. Intracellular Ca^{2+} levels in H9C2 cardiomyocytes were markedly increased in the H/R group, whereas ERO1α knockdown decreased the intracellular Ca^{2+} levels (Fig. 5A and B). Furthermore, oxidative stress is related to apoptosis-induced H/R injury (28), thus intracellular ROS levels were analyzed to investigate the association between ERO1α and oxidative stress. ERO1α knockdown significantly decreased intracellular ROS levels in the H/R group (Fig. 5C).

ERO1α knockdown alleviates H/R-induced mitochondrial dysfunction through reducing ERS. To investigate whether ERO1α knockdown protected mitochondrial function in H/R injury, cardiomyocytes were pretreated with 2 μg/l TM, an ERS activator, 24 h prior to H/R exposure to counteract the reduction in ERS following ERO1α knockdown. Intracellular ROS levels, $\Delta\psi$m, and expression levels of cytochrome c in mitochondrial and cytosolic fractions were evaluated. TM pretreatment of ERO1α-shRNA-transfected H9C2 cardiomyocytes undergoing H/R injury did not reverse the reduction in intracellular ROS levels observed following ERO1α knockdown (Fig. 5C). Compared with the H/R group, decreased expression levels of cytochrome c were observed in the cytoplasm in the ERO1α-shRNA + H/R group, whereas increased levels were found in the mitochondria. However, no significant differences were observed between the TM + ERO1α-shRNA + H/R and the ERO1α-shRNA + H/R groups (Fig. 6A). After H/R, the $\Delta\psi$m significantly decreased, while ERO1α knockdown had a trend towards an increase in $\Delta\psi$m in the ERO1α-shRNA + H/R group; however, there was no significant difference when comparing the H/R and ERO1α-shRNA + H/R groups (Fig. 6B). Taken together, these findings suggested that ERO1α may be responsible for the H/R-induced mitochondrial damage of H9C2 cardiomyocytes, which is associated with ERS.

Discussion

In mammalian cells, the ER has an important role in the proper folding and assembly of polypeptide chains, Ca^{2+} storage and post-translational modifications (29). ERS occurs following I/R-induced increases in ROS, which results in the accumulation of misfolded or unfolded proteins in the ER lumen (30). Thus, there is increasing evidence to suggest that ERS is associated with I/R injury (31-33).

ERO1α is a conserved glycoprotein, which has been demonstrated to accept electrons from reduced protein disulfide isomerase and transfer them to oxygen molecules, catalyze the formation of oxygen-mediated protein disulfide bonds and contribute to ERS (34,35). ERO1α activity may be an important factor contributing to the large production of ROS in cells, as it has been previously found that ERO1α dysfunction may result in a rapid decrease in ER-derived oxidative stress (16). However, in homocysteine-induced ERS, ERO1α demonstrated a negative regulatory effect (36). In the present study, ERO1α expression levels in H9C2 cardiomyocytes were confirmed using western blotting, and H/R induction was subsequently used to simulate I/R in these cells to further verify whether ERO1α expression was altered as a result of oxidative stress. ERO1α expression levels in H9C2 cardiomyocytes were markedly increased following H/R, reaching their highest levels following 6 h of reoxygenation, whereas 4-PBA decreased the expression levels. In addition, the number of apoptotic cells was significantly increased following H/R induction. Therefore, it was hypothesized that ERO1α may serve an important role in H/R development.

To further understand ERO1α function in H9C2 cardiomyocytes following H/R, lentiviral shRNA was used to reduce ERO1α expression levels. In previous studies, it has been reported that following myocardial I/R, ERS promoted apoptosis in cardiomyocytes through the CHOP and caspase-12 signaling pathways (37); that c-caspase-12 expression levels, and caspase-3 activity were increased following H/R (38,39); and that caspase-12, which indirectly activates cytoplasmic caspase-3, was considered to be a crucial mediator of ERS-induced apoptosis (40). Consistent with these studies, the data from the present study revealed that the expression levels of GRP78, CHOP and c-caspase-12, as well as caspase-3 activity, were significantly increased. However, following the transfection of H9C2 cardiomyocytes with ERO1α-shRNA, the expression levels and activity significantly decreased. These results indicated that ERO1α may have an important role in ERS, and that the downregulation of ERO1α may decrease ERS and apoptosis in myocardial cells following H/R injury.

The ER is the main storage location of Ca^{2+} in cells and participates in dynamic Ca^{2+} exchange with the mitochondria (41); Ca^{2+} is transferred to the mitochondrial matrix to stimulate mitochondrial ATP synthesis by activating the tricarboxylic acid cycle. During I/R, the increase in intracellular ROS levels and oxidative stress from multiple different sources leads to a large amount of Ca^{2+} dissociating from the ER to the mitochondria (42). This subsequently promotes mitochondrial Ca^{2+} overload, which triggers cell apoptosis by opening the mitochondrial permeability transition pore (43). Oxidative stress promotes ERS, and persistent ERS has been observed to promote mitochondrial dysfunction, which in turn induces oxidative stress (44). As previously mentioned, ERO1α is strongly associated with the generation of ROS, and it has been demonstrated that due to excessive oxidation, ERO1α enhances inositol triphosphate receptor (IP3R) activity, and promotes IP3R-mediated Ca^{2+} release and transfer to the mitochondria, facilitating apoptosis (45,46). Thus, further investigation into the relationship between ERO1α and mitochondrial function following H/R is required.

The $\Delta\psi$m reflects the functional status of the mitochondria. In the present study, it was observed that oxidative stress

led to a decrease in Δψm, accompanied by significantly increased ERO1α expression levels. Compared with the H/R group, following ERO1α-shRNA transfection, the concentration of Ca^{2+} decreased, while ERO1α knockdown had a trend towards an increase in Δψm. ERO1α knockdown reduced the release of cytochrome c from the mitochondria to the cytoplasm. However, the pretreatment of ERO1α-transfected H9C2 cardiomyocytes with TM following H/R injury did not reverse the reduced intracellular ROS levels, the ratio of cytoplasmic/mitochondrial cytochrome c achieved by ERO1α knockdown. These results suggested that the downregulation of ERO1α may attenuate oxidative stress, and decrease the intracellular Ca^{2+} concentration and the percentage of apoptotic cells in H9C2 cardiomyocytes following H/R.

In conclusion, the findings in the present study indicated that ERO1α may serve as a positive mediator of the apoptotic pathway during H/R; however, the exact mechanism by which ERO1α achieves this function remains to be investigated. In addition, the effects of ERO1α on the H9C2 cardiomyocytes *in vitro* may not reflect the *in vivo* scenario; thus, future studies should encompass animal models for further validation of these results.

Acknowledgements

Not applicable.

Funding

This study was supported by the Science and Technology Innovation Team Project of Changzhi Medical College (grant no. CX201409).

Availability of data and materials

The datasets used and/or analyzed during the current study are available from the corresponding author on reasonable request.

Authors' contributions

LNL and XJZ conceived and designed the experiments; YL, YYL, SLC and NZ performed the experiments; and DW and LNL were involved in analyzing the data and drafting the manuscript. All authors read and approved the final manuscript.

Ethics approval and consent to participate

Not applicable.

Patient consent for publication

Not applicable.

Competing interests

The authors declare that they have no competing interests.

References

1. Braunwald E and Kloner RA: Myocardial reperfusion: A double-edged sword? J Clin Invest 76: 1713-1719, 1985.
2. Hausenloy DJ and Yellon DM: Ischaemic conditioning and reperfusion injury. Nat Rev Cardiol 13: 193-209, 2016.
3. Hausenloy DJ and Yellon DM: Myocardial ischemia-reperfusion injury: A neglected therapeutic target. J Clin Invest 123: 92-100, 2013.
4. Dhalla NS, Elmoselhi AB, Hata T and Makino N: Status of myocardial antioxidants in ischemia-reperfusion injury. Cardiovasc Res 47: 446-456, 2000.
5. Chang JC, Lien CF, Lee WS, Chang HR, Hsu YC, Luo YP, Jeng JR, Hsieh JC and Yang KT: Intermittent hypoxia prevents myocardial mitochondrial Ca^{2+} overload and cell death during ischemia/reperfusion: The role of reactive oxygen species. Cells 8: E564, 2019.
6. Farrukh MR, Nissar UA, Afnan Q, Rafiq RA, Sharma L, Amin S, Kaiser P, Sharma PR and Tasduq SA: Oxidative stress mediated Ca (2+) release manifests endoplasmic reticulum stress leading to unfolded protein response in UV-B irradiated human skin cells. J Dermatol Sci 75: 24-35, 2014.
7. Martindale JJ, Fernandez R, Thuerauf D, Whittaker R, Gude N, Sussman MA and Glembotski CC: Endoplasmic reticulum stress gene induction and protection from ischemia/reperfusion injury in the hearts of transgenic mice with a tamoxifen-regulated form of ATF6. Circ Res 98: 1186-1193, 2006.
8. Jian L, Lu Y, Lu S and Lu C: Chemical chaperone 4-phenylbutyric acid reduces cardiac ischemia/reperfusion injury by alleviating endoplasmic reticulum stress and oxidative stress. Med Sci Monit 22: 5218-5227, 2016.
9. Kerkhofs M, Giorgi C, Marchi S, Seitaj B, Parys JB, Pinton P, Bultynck G and Bittremieux M: Alterations in Ca^{2+} signalling via ER-mitochondria contact site remodelling in cancer. Adv Exp Med Biol 997: 225-254,2017.
10. Kerkhofs M, Bittremieux M, Morciano G, Giorgi C, Pinton P, Parys JB and Bultynck G: Emerging molecular mechanisms in chemotherapy: Ca^{2+} signaling at the mitochondria-associated endoplasmic reticulum membranes. Cell Death Dis 9: 334, 2018.
11. Morciano G, Marchi S, Morganti C, Sbano L, Bittremieux M, Kerkhofs M, Corricelli M, Danese A, Karkucinska-Wieckowska A, Wieckowski MR, *et al*: Role of mitochondria-associated ER membranes in calcium regulation in cancer-specific settings. Neoplasia 20: 510-523, 2018.
12. Dias-Gunasekara S, Gubbens J, van Lith M, Dunne C, Williams JA, Kataky R, Scoones D, Lapthorn A, Bulleid NJ and Benham AM: Tissue specific expression and dimerization of the endoplasmic reticulum oxidoreductase Ero1beta. J Biol Chem 280: 33066-33075, 2005.
13. Zito E, Chin KT, Blais J, Harding HP and Ron D: ERO1-beta, a pancreas-specific disulfide oxidase, promotes insulin biogenesis and glucose homeostasis. J Cell Biol 188: 821-832, 2010.
14. Pagani M, Fabbri M, Benedetti C, Fassio A, Pilati S, Bulleid NJ, Cabibbo A and Sitia R: Endoplasmic reticulum oxidoreductin 1-Lbeta (ERO1-Lbeta), a human gene induced in the course of the unfolded protein response. J Biol Chem 275: 23685-23692, 2000.
15. Gess B, Hofbauer KH, Wenger RH, Lohaus C, Meyer HE and Kurtz A: The cellular oxygen tension regulates expression of the endoplasmic oxidoreductase ERO1-Lalpha. Eur J Biochem 270: 2228-2235, 2003.
16. Sevier CS and Kaiser CA: Ero1 and redox homeostasis in the endoplasmic reticulum. Biochim Biophys Acta 1783: 549-556, 2008.
17. Seervi M, Sobhan PK, Joseph J, Ann Mathew K and Santhoshkumar TR: ERO1α-dependent endoplasmic reticulum-mitochondrial calcium flux contributes to ER stress and mitochondrial permeabilization by procaspase-activating compound-1 (PAC-1). Cell Death Dis 4: e968, 2013.
18. Nakamura K, Tamaki H, Kang MS, Mochimaru H, Lee ST, Nakamura K and Kamagata Y: A six-well plate method: Less laborious and effective method for cultivation of obligate anaerobic microorganisms. Microbes Environ 26: 301-306, 2011.
19. Li J, Xia X, Ke Y, Nie H, Smith MA and Zhu X: Trichosanthin induced apoptosis in HL-60 cells via mitochondrial and endoplasmic reticulum stress signaling pathways. Biochim Biophys Acta 1770: 1169-1180, 2007.
20. Lai LN, Zhang XJ, Zhang XY, Song LH, Guo CH, Lei JW and Song XL: Lazaroid U83836E protects the heart against ischemia reperfusion injury via inhibition of oxidative stress and activation of PKC. Mol Med Rep 13: 3993-4000, 2016.

21. Lai L, Chen Y, Tian X, Li X, Zhang X, Lei J, Bi Y, Fang B and Song X: Artesunate alleviates hepatic fibrosis induced by multiple pathogenic Factors and inflammation through the inhibition of LPS/TLR4/NF-κB signaling pathway in rats. Eur J Pharmacol 765: 234-241, 2015.
22. Livak KJ and Schmittgen TD: Analysis of relative gene expression data using real-time quantitative PCR and the 2(-Delta Delta C(T)) method. Methods 25: 402-408, 2001.
23. Wu H, Ye M, Yang J and Ding J: Modulating endoplasmic reticulum stress to alleviate myocardial ischemia and reperfusion injury from basic research to clinical practice: A long way to go. Int J Cardiol 223: 630-631, 2016.
24. Yu L, Li S, Tang X, Li Z, Zhang J, Xue X, Han J, Liu Y, Zhang Y, Zhang Y, *et al*: Diallyl trisulfide ameliorates myocardial ischemia-reperfusion injury by reducing oxidative stress and endoplasmic reticulum stress-mediated apoptosis in type 1 diabetic rats: Role of SIRT1 activation. Apoptosis 22: 942-954, 2017.
25. Yoon S, Park SJ, Han JH, Kang JH, Kim JH, Lee J, Park S, Shin HJ, Kim K, Yun M and Chwae YJ: Caspase-dependent cell death-associated release of nucleosome and damage-associated molecular patterns. Cell Death Dis 5: e1494, 2014.
26. Groenendyk J, Sreenivasaiah PK, Kim DH, Agellon LB and Michalak M: Biology of endoplasmic reticulum stress in the heart. Circ Res 107: 1185-1197, 2010.
27. Weiss JN, Korge P, Honda HM and Ping P: Role of the mitochondrial permeability transition in myocardial disease. Circ Res 93: 292-301, 2003.
28. Kalogeris T, Baines CP, Krenz M and Korthuis RJ: Cell biology of ischemia/reperfusion injury. Int Rev Cell Mol Biol 298: 229-317, 2012.
29. Gelebart P, Opas M and Michalak M: Calreticulin, a Ca^{2+}-binding chaperone of the endoplasmic reticulum. Int J Biochem Cell Biol 37: 260-266, 2005.
30. Doroudgar S and Glembotski CC: New concepts of endoplasmic reticulum function in the heart: Programmed to conserve. J Mol Cell Cardiol 55: 85-91, 2013.
31. Guan G, Zhang J, Liu S, Huang W, Gong Y and Gu X: Glucagon-like peptide-1 attenuates endoplasmic reticulum stress-induced apoptosis in H9c2 cardiomyocytes during hypoxia/reoxygenation through the GLP-1R/PI3K/Akt pathways. Naunyn Schmiedebergs Arch Pharmacol 392: 715-722, 2019.
32. Wang XB, Huang XM, Ochs T, Li XY, Jin HF, Tang CS and Du JB: Effect of sulfur dioxide preconditioning on rat myocardial ischemia/reperfusion injury by inducing endoplasmic reticulum stress. Basic Res Cardiol 106: 865-878, 2011.
33. Xu J, Hu H, Chen B, Yue R, Zhou Z, Liu Y, Zhang S, Xu L, Wang H and Yu Z: Lycopene protects against hypoxia/reoxygenation injury by alleviating ER stress induced apoptosis in neonatal mouse cardiomyocytes. PLoS One 10: e0136443, 2015.
34. Zito E: ERO1: A protein disulfide oxidase and H2O2 producer. Free Radic Biol Med 83: 299-304, 2015.
35. Zeeshan HM, Lee GH, Kim HR and Chae HJ: Endoplasmic reticulum stress and associated ROS. Int J Mol Sci 17: 327, 2016.
36. Yang X, Xu H, Hao Y, Zhao L, Cai X, Tian J, Zhang M, Han X, Ma S, Cao J and Jiang Y: Endoplasmic reticulum oxidoreductin 1α mediates hepatic endoplasmic reticulum stress in homocysteine-induced atherosclerosis. Acta Biochim Biophys Sin (Shanghai) 46: 902-910, 2014.
37. Neuber C, Uebeler J, Schulze T, Sotoud H, El-Armouche A and Eschenhagen T: Guanabenz interferes with ER stress and exerts protective effects in cardiac myocytes. PLoS One 9: e98893, 2014.
38. Zhu X, Zhang ZL, Li P, Liang WY, Feng XR and Liu ML: Shenyuan, an extract of American ginseng and corydalis tuber formula, attenuates cardiomyocyte apoptosis via inhibition of endoplasmic reticulum stress and oxidative stress in a porcine model of myocardial infarction. J Ethnopharmacol 150: 672-681, 2013.
39. Mei Y, Thompson MD, Shiraishi Y, Cohen RA and Tong X: Sarcoplasmic/endoplasmic reticulum Ca^{2+} ATPase C674 promotes ischemia- and hypoxia-induced angiogenesis via coordinated endothelial cell and macrophage function. J Mol Cell Cardiol 76: 275-282, 2014.
40. Szegezdi E, Fitzgerald U and Samali A: Caspase-12 and ER-stress-mediated apoptosis: The story so far. Ann NY Acad Sci 1010: 186-194, 2003.
41. Giorgi C, De Stefani D, Bononi A, Rizzuto R and Pinton P: Structural and functional link between the mitochondrial network and the endoplasmic reticulum. Int J Biochem Cell Biol 41: 1817-1827, 2009.
42. Park SJ, Lee SB, Suh Y, Kim SJ, Lee N, Hong JH, Park C, Woo Y, Ishizuka K, Kim JH, *et al*: DISC1 modulates neuronal stress responses by gate-keeping ER-mitochondria Ca^{2+} transfer through the MAM. Cell Rep 21: 2748-2759, 2017.
43. Marchi S, Bittremieux M, Missiroli S, Morganti C, Patergnani S, Sbano L, Rimessi A, Kerkhofs M, Parys JB, Bultynck G, *et al*: Endoplasmic reticulum-mitochondria communication through Ca^{2+} signaling: The importance of mitochondria-associated membranes (MAMs). Adv Exp Med Biol 997: 49-67, 2017.
44. Yang L, Guan G, Lei L, Liu J, Cao L and Wang X: Oxidative and endoplasmic reticulum stresses are involved in palmitic acid-induced H9c2 cell apoptosis. Biosci Rep 39: BSR20190225, 2019.
45. Kang S, Kang J, Kwon H, Frueh D, Yoo SH, Wagner G and Park S: Effects of redox potential and Ca^{2+} on the inositol 1,4,5-trisphosphate receptor L3-1 loop region: Implications for receptor regulation. J Biol Chem 283: 25567-25575, 2008.
46. Li G, Mongillo M, Chin KT, Harding H, Ron D, Marks AR and Tabas I: Role of ERO1-alpha-mediated stimulation of inositol 1,4,5-triphosphate receptor activity in endoplasmic reticulum stress-induced apoptosis. J Cell Biol 186: 783-792, 2009.